



Research Article
Mutagenesis

Lack of genotoxicity of iron oxide maghemite ($\gamma\text{-Fe}_2\text{O}_3$) and magnetite (Fe_3O_4) nanoparticles to *Oreochromis niloticus* after acute exposures

Maria Luiza Fascineli², Paolin Rocio Cáceres-Vélez¹, Willie Oliveira Pinheiro¹, Sacha Braun Chaves¹, Marcelo Henrique Sousa³, Wilson Sacchi Peternella⁴, Frederico Hillesheim Horst¹, Michele de Castro Fernandes¹, Wania Guimarães¹ , Ricardo Bentes Azevedo¹ and Cesar Koppe Grisolia¹ 

¹Universidade de Brasília, Instituto de Ciências Biológicas, Departamento de Genética e Morfologia, Brasília, DF, Brazil.

²Universidade Federal da Paraíba, Centro de Ciências da Saúde, Departamento de Morfologia, João Pessoa, PB, Brazil.

³Universidade de Brasília, Faculdade de Ceilândia, Brasília, DF, Brazil.

⁴Universidade Federal de Rondônia, Departamento de Química, Porto Velho, RO, Brazil.

Abstract

Iron oxide nanoparticles (FeO-NPs) are widely used in scientific and technological fields. Environmental concerns have been raised about residual FeO-NPs levels as their toxicity and bioaccumulative potential are not well understood. *Oreochromis niloticus* were exposed to nanoparticles of $\gamma\text{-Fe}_2\text{O}_3$ and Fe_3O_4 . Micro-CT 3D image and grayscale graphic assessments revealed the accumulation of radiopaque material in the digestive tract of fish exposed to FeO-NPs. Histological analysis showed the presence of such NPs in the hepatopancreas, gills, kidneys, and muscles. No genotoxicity occurred, through micronucleus test and comet assay in peripheral erythrocytes. Body clearance was confirmed by iron-content reduction in organisms exposed to FeO-NPs after recovery period. No tissue injuries were observed in the exposed animals which may be attributed to the absence or low toxicity of iron oxide nanoparticles under the study conditions. *O. niloticus* showed tolerance to sublethal exposures to FeO-NPs.

Keywords: Magnetite, maghemite, tilapia fish, nanotoxicology, nanoparticles.

Received: November 19, 2023; Accepted: July 23, 2024.

Introduction

Nanotechnology is a major innovative scientific and economic growth area (Farré *et al.*, 2009) comprising the study, manipulation, construction materials, substances, devices and objects that have exhibit specific properties relating to nanoscale (Ostiguy *et al.*, 2009). The exponential growth of nanotechnology can introduce a considerable amount of new nanomaterials (NMs) into the environment (Oberdörster *et al.*, 2005), that may affect aquatic/terrestrial organisms and have a detrimental impact on human health (Nowack and Bucheli, 2007). Once released into the environment, engineered nanomaterials can aggregate to some degree, possibly associating with suspended solids and sediment. They may even be accumulated by organisms after entering drinking water sources and food materials (Boxall *et al.*, 2007), the environmental and/or health consequences of which are not fully understood.

Among the commercially available nanomaterials, one can include the metal oxides, *e.g.* TiO_2 , aluminum oxides and iron oxides. Iron oxide nanoparticles (FeO-NPs) have wide applications in industry, the environment and biomedicine. These applications are correlated with specific size, shape,

surface characteristics, and especially magnetic properties (Teja and Koh, 2009), as observed in maghemite ($\gamma\text{-Fe}_2\text{O}_3$) and magnetite (Fe_3O_4).

Increased commercial use of iron oxide nanoparticles could result in their release into the environment and aquatic ecosystems in large quantities posing risks to aquatic and/or terrestrial organisms (Ates *et al.*, 2016). Research into the associated ecological impacts and health risks is limited because FeO-NPs are generally considered to present little or no toxicity (Zhang *et al.*, 2015; Ali *et al.*, 2016). However, there is scientific literature documenting the production of reactive oxygen species (ROS) (Patil *et al.*, 2015) after exposure to FeO-NPs with the ability to stimulate cell membrane lipid peroxidation, promoting toxic effects (Valdiglesias *et al.*, 2015). Moreover, FeO-NPs could serve as significant carriers of toxic environmental chemicals and increase exposure to adsorbed pollutants (Zhang *et al.*, 2015).

The ability to recognize potentially harmful *in vivo* effects after exposure to metallic nanoparticles, including FeO-NPs, is indispensable given their broad use. In general, metal pollution has constituted an environmental issue in many developed and developing countries for decades. Therefore, there remains a substantial need to not only understand the bioaccumulation and toxicity of metals in aquatic organisms (Wang and Rainbow, 2008), but also to better understand these effects in relation to NMs and identify any possible toxicity resulting from exposure/accumulation.

Send correspondence to Cesar Koppe Grisolia. Universidade de Brasília, Instituto de Ciências Biológicas, Departamento de Genética e Morfologia, Campus Darcy Ribeiro, 70910-900, Brasília, DF, Brazil. E-mail: grisolia@unb.br.

In general, both acute and chronic toxicity tests are used to verify material safety and identify any lethal/sublethal effects resulting from its aquatic exposure. In acute toxicity tests, fish are usually exposed to the test item for 96 h. Clinical and behavioral abnormalities, morbidity and mortality are recorded, together with the determination of the lethal concentration, based on recommended OECD protocol for fish acute toxicity test number 203 (OECD, 2019). Although chronic studies (>7 days) are more realistic about the concentrations of chemicals found in the environment, acute aquatic toxicity testing remains a basic requirement for chemical registration in most countries (Elijah *et al.*, 2015). Acute toxicity represents a key property in defining the hazard of large quantities of a substance in cases of accidents or major spillages (GHS, 2019).

An environmental risk assessment is required to provide information about exposure levels and the hazard(s) that a chemical poses to organisms, with the same assessment paradigm used for NM appraisal (Brink *et al.*, 2019). In addition, some authors suggest that evaluations of uptake, biodistribution, and clearance are useful endpoints for characterizing exposure to NMs and their interaction with biota (Pomeren *et al.*, 2017). Brink *et al.* (2019) considered that the evaluation and quantification of absorption and elimination by organisms are essential in NM environmental risk assessments. However, there are still many uncertainties about how to analyze the toxicological potential of NMs.

Therefore, in this study we examined the intake, uptake, accumulation, and the elimination of FeO-NPs (γ -Fe₂O₃ and Fe₃O₄), together with genotoxicity evaluations in a tilapia fish (*Oreochromis niloticus*) after acute exposures. Recovery test was also carried out with the understanding how an aquatic organism manages the environmental risks of nanomaterials.

Material and Methods

Synthesis and characterization of iron oxide nanoparticles

FeO-NPs were prepared in accordance with the procedure described by Peternele *et al.* (2014). Briefly, magnetite (Fe₃O₄) nanoparticles were synthesized by co-precipitation of Fe³⁺ and Fe²⁺ ions in an alkaline solution. The resulting precipitate was washed until neutral pH and dried at 40 °C for 24 h. Maghemite (γ -Fe₂O₃) nanoparticles were obtained by oxidation of the as-prepared magnetite powder for 3 h at 250 °C, in air atmosphere.

Crystallographic analysis of the samples was performed using the X-ray powder diffraction (XRD) method. Diffraction patterns (20 degrees) were recorded by a Bruker AXL Mod. D8 diffractometer equipped with a copper cathode (Cu K α_1 1,5418 Å) and Ni filter, operating at 40 kV and a current of 20 mA. A continuous scan of 2 deg/min mode was used to collect 20 data from 20 to 70 degrees. An X-ray diffractogram was plotted with the aid of the Microcal Origin 6.0 software (Microcal Software Inc., Northampton, MA, USA). The full width at half maximum of the (311) reflection was used for particle size determination together with the Scherrer equation (Morais *et al.*, 2001). FeO-NPs morphology were evaluated by Transmission Electron Microscopy (TEM) using a JEM-2100F microscope (Tokyo, Japan). For Principal Group the

concentration of 25 and 50 mg/L were also evaluated for some parameters

In vivo studies

Young adult *Oreochromis niloticus* (Tilapia) fish were obtained from a local fish farm (NUPISC/ SEAGRI-DF, Brasilia, Brazil) where breeding and sanitary conditions were constantly monitored and controlled. Fish of approximately 9±2 cm in length were used in the Principal Group (PG), in which fishes were exposed to FeO-NPs for 24 or 96 h (exposure phase). Animals were subsequently euthanized. The Satellite Group (SG) animals were exposed to FeO-NPs for 96 h, after which time the water was replaced with fresh water without NMs (recovery time) for a further 96 or 192 h. Both the PG and SG consisted of 3 subgroups (control, Fe₃O₄ and γ -Fe₂O₃) with a maximum of 8 fish for each time period (24, 96, 192 or 288 h) and were exposed to FeO-NPs at 0 mg/L (control group), 100 mg/L (Fe₃O₄) or 100 mg/L (γ -Fe₂O₃).

Throughout the experimental phase, all fish were housed in aquariums with: photoperiods of 10 h light/14 h dark, pH 7.5 ± 0.5, constant aeration, and 26 ± 1 °C, with water changed every 96 h. The animals received commercial food once a day in the morning, except during the 96-h exposure phase or 192 and 288 h post-exposure phase. Physicochemical parameters, such as dissolved oxygen, nitrites and ammonia, were measured pre- and post-exposure using commercial kits (Labcon®) and conductivity (PHTEKCD203). All parameters remained within the value ranges proposed by the OECD guideline 203 (2019).

Genotoxic evaluations – micronucleus test and comet assay

Peripheral erythrocytes of *Oreochromis niloticus* were used to detect genotoxic effects caused by exposure to γ -Fe₂O₃ or Fe₃O₄ after 96 hours of exposure, followed or not by a period without exposure, to verify possible recovery or late effects from tested nanoparticles. Peripheral erythrocytes were collected and evaluated for the formation of micronuclei and nuclear abnormalities, as well as for comet assay after exposures at 0.0, 25.0, 50.0 and 100.0 mg/L of both NPs. In the satellite groups, exposures occurred only at 100.0 mg/L at 192 and 288 h, to follow the recovery group.

For micronucleus, nuclear abnormalities and comet assay, peripheral blood samples were homogenized in 1 mL of fetal bovine calf and low melt agarose respectively. From this sample, 0.5 mL were used for smear in the micronucleus (MN) and nuclear abnormalities (NA) study. 2000 erythrocytes were scored for MN and 2000 for NA at 1000 magnification, and they were evaluated under a blind code. Erythrocytes were also scored to classify nuclear abnormalities such as BB - blebbed, LB - lobed, NT - notched, BN - binucleated and NB - nuclear bud (Al-Sabti and Metcalfe, 1995). For comet assay - alkaline test blood samples were homogenized in 100 μ L of low melt agarose at 0.5% at 37 °C, then these samples were distributed on microscope slides, and covered with a coverslip of 60 mm. The slides were kept in lyse solution for 1 h at 4 °C, and electrophoresis occurred at 0.85 V/cm and 4 °C for 15 min. The cell (nucleoid) analysis for comet classifications followed the protocol developed by Singh *et al.* (1988), with

modifications. One hundred nucleoids per fish were analyzed (blind analysis) and classified based on tail length. During the exposure and post-exposure phases, mortality, clinical signs, and behavioral changes were recorded, twice a day. After exposure, or the post-exposure phase, animals were euthanized with 1% benzocaine hydrochloride in the water. Fish and tissue fragments were subsequently processed.

High-resolution X-ray microtomography (micro-CT)

Three animals from each group were euthanized 24, 96 (PG) and 192 h (SG), placed in Davidson's fixative solution for 24 h and stored in 70% alcohol. Three-dimensional computerized microtomography images of tilapia fish exposed (or not) to FeO-NPs were obtained to evaluate the fate of metals in the body.

Tilapia fish were scanned in a Skyscan 1076 MicroCT (Skyscan, Kontich, Belgium) at 50 kV, 141 μ A, Al 0.5 mm filter and 12.56 pixel size. Reconstruction was performed using NRecon software (Skyscan, Kontich, Belgium), applying smoothing, beam-hardening and ring-artifact correction at 01, 10 and 07 level, respectively. Grayscale range was set from 0.2386 to 0.103696 HU. The reconstructed MicroCT files were used to analyze the samples and to create volume renderings of the region of interest, using the CT-Analyzer software (Skyscan, Kontich, Belgium).

Inductively coupled plasma optical emission spectrometry (ICP-OES)

Quantitative analysis of FeO-NP biodistribution, by means of the dosage of iron content in biological material, was performed with inductively coupled plasma optical emission spectrometry (ICP-OES) using an Optima™ 8000 ICP-OES Spectrometer. Sample preparation involved a tissue fragment of each fish (gill, hepatopancreas, kidney and muscle) and collection of an aliquot of the blood of 5 fish which were weighed and frozen at the end of the exposure (96 h) or recovery time (192 or 288 h). These samples were subsequently dried using an Integrated SpeedVac® System, SAVANT SPD2010 (Thermo Electron Corporation, Milford, MA, US). The dried samples were submitted to acid digestion using nitric acid (70% HNO₃) for 48 h at RT, as proposed in the literature (Ashoka *et al.*, 2009; Sousa *et al.*, 2011). After diluting samples with ultrapure water, the iron content was measured by ICP-OES and expressed as mg Fe/kg of fresh tissue for all tissues.

Perl's Prussian Blue Staining

Gill, hepatopancreas and intestine tissue fragments of the same 5 fish utilized in ICP-OES were fixed, dehydrated and embedded in paraffin. Samples were cut with a microtome (LEICA RM2235), stained with Perl's Prussian Blue, and analyzed by optical microscopy (ZEISS Axioskop 2-HAL 100), to detect the presence of iron.

Statistical analyses

Differences between control and treated groups for quantitative data were performed with parametric or non-

parametric tests according to normality distribution, e.g., ANOVA (F) or Kruskal-Wallis (H) tests, respectively, followed or not by *post-hoc* analysis (Dunnett's or Dunn's Methods). Differences between treated groups for different NPs at the same time were analyzed with the *t*-Test or Mann-Whitney test according to normality distribution. Qualitative data were assessed using the Chi-square Test. Analyses were performed by the IBM SPSS Statistics for Windows, Version 20.0 (2011) program.

Ethics

The project was approved by the Ethics Committee of the University of Brasilia (Protocol 79/2017).

Results

Nanomaterial characterization

In the present study, nanoparticles were characterized by XRD (Figure 1) and TEM (Figure 2). After coprecipitation of iron salts, a black powder was obtained, indicating formation of the Fe₃O₄ phase. The XRD pattern of this sample is shown in Figure 1, with the peaks of the recorded diffractogram readily indexed to the magnetite phase (JCPDS 19-0629). After magnetite oxidation, a reddish-brown precipitate indicative of the conversion of magnetite to maghemite was obtained. The diffracted peaks of this sample were indexed to the γ -Fe₂O₃ structure (JCPDS 39-1346) in the pattern shown in Figure 1. The magnetite and maghemite XRD peaks are very analogous; however, as shown in Figure 1, for the oxidized sample, the equivalent XRD peaks are slightly shifted towards the higher angles indicating the predominance of the maghemite phase. More specifically, the quantitative shift of the (511) XRD peak towards 57.5° indicates complete conversion of magnetite into maghemite (Silva *et al.*, 2017). Using Scherrer's formula to broaden the (311) XRD line, the average crystalline sizes of the Fe₃O₄ and γ -Fe₂O₃ samples were estimated to be 9.0 and 8.0 nm, respectively.

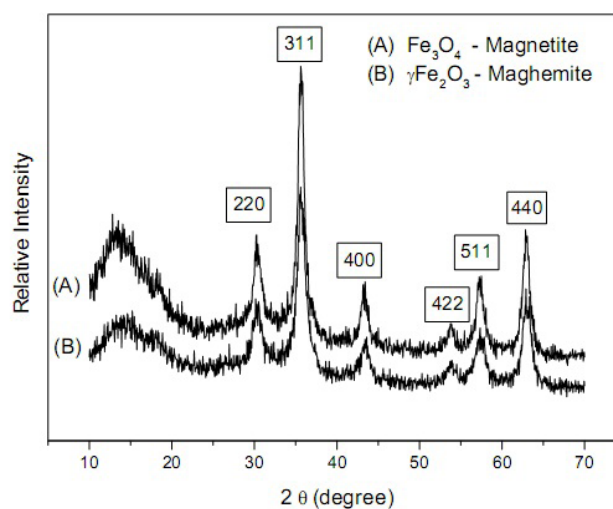


Figure 1 – XRD patterns of the magnetite (Fe₃O₄) nanoparticles by coprecipitation (A), and maghemite (γ -Fe₂O₃) nanoparticles (B).

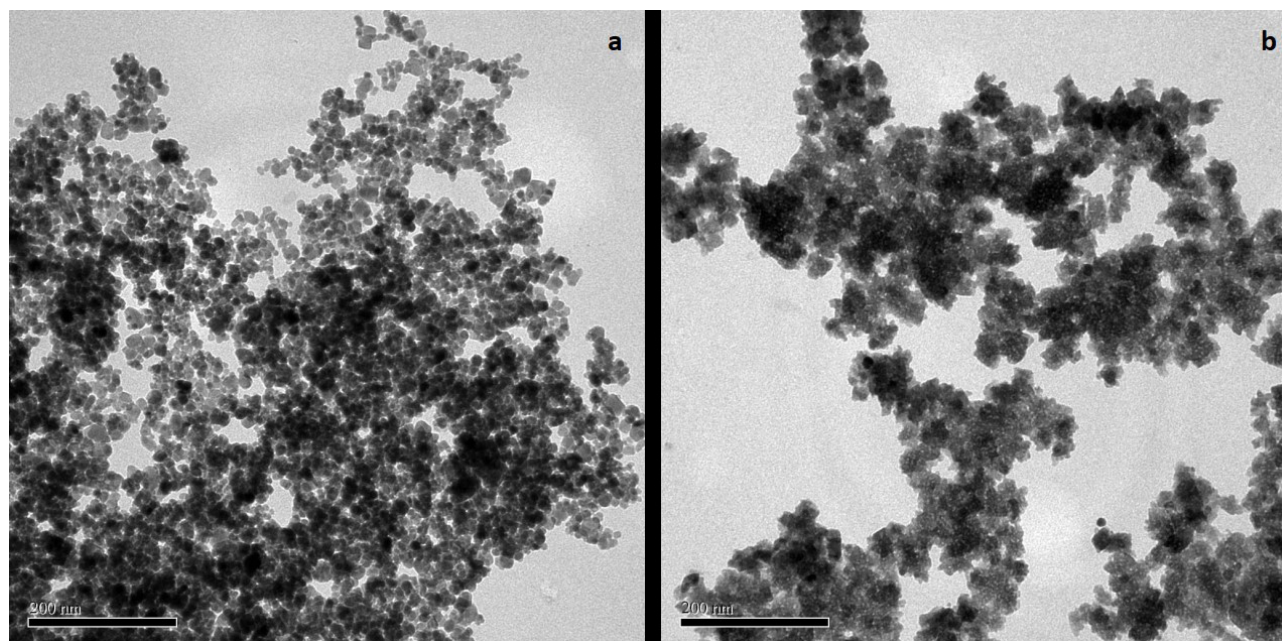


Figure 2 – Transmission Electron Microscopy: a) maghemite ($\gamma\text{-Fe}_2\text{O}_3$) and b) magnetite (Fe_3O_4).

The TEM images of FeO-NPs in Figure 1 show that the magnetite and maghemite NPs present an almost spherical morphology and are polydisperse in size, as previously observed for this route of synthesis (Peternele *et al.*, 2014).

Genotoxicity

Mortality, clinical signs and behavioral changes were not observed during the exposure and post-exposure phases. Mutagenic effects (Table 1) were not statistically significant for Principal Group (Np- $\gamma\text{-Fe}_2\text{O}_3$ (H = 10.546 – p = 0.014 and post test p > 0.05); Np- Fe_3O_4 (H = 3.474 – p = 0.324) or Satellite Group (H = 0.692 and p = 0.708) in the recovery time of the 192 h to subgroups exposed to iron oxide nanoparticles compared with control group. However, in the 288 h of the recovery time (H = 8.222 and p = 0.016) the exposure to Np- Fe_3O_4 was statistically significant (p < 0.05) for occurrence of micronucleus.

The exposed groups ($\gamma\text{-Fe}_2\text{O}_3$ or Fe_3O_4) were evaluated in relation to the control group of each subgroup; whose statistical differences are represented by an asterisk (*), p < 0.05. Data are represented by mean \pm standard deviation (%). Principal Group – 96 hours post exposure of the test item; Satellite Group – 96 hours post exposure of the test item plus 96 or 192 hours of the additional recovery period (Total - 192 or 288 hours, respectively).

For cytotoxic effects (Table 1), the occurrence of bud nucleus cells in subgroup 50 mg/L after exposure to Np- Fe_3O_4 was statistically significant (H = 15.144 – p < 0.05), but this was considered a biological finding without toxicological relevance. Other findings were observed as lobed erythrocyte nuclei after exposure to 50 or 100 mg/L of the Np- Fe_3O_4 in Principal Group (H = 11.447 and p = 0.010; post hoc test p < 0.05), as well as in the Satellite Group at 288 h (H = 8.789 and p = 0.012; post hoc test p < 0.05), when compared control

groups with Np- Fe_3O_4 . The exposure to the test item promoted a reduction in the frequency of the notched nucleus cells at Principal Group (Np- $\gamma\text{-Fe}_2\text{O}_3$ - 50 and 100 mg/L) and Satellite Group (Np- Fe_3O_4 - 100 mg/L) when compared with the control group (H = 14.259 and p = 0.003; H = 8.084 and p = 0.018, respectively; post hoc test p < 0.05 – for both). However, the frequency of notched nucleus cells was variable in our groups, in this way, this biological finding was considered without toxicological relevance.

The comet assay showed that there was no statistically significant difference in DNA damage, as represented in Figure 8. The exposure to Np- $\gamma\text{-Fe}_2\text{O}_3$ (H = 7.074 – p = 0.070) or to Np- Fe_3O_4 (F = 0.857 – p = 0.479) for 96 h was not enough to promote DNA fragmentation. No late effects were observed either, during the recovery period (192 and 288 hours), resulting from exposure to Np- $\gamma\text{-Fe}_2\text{O}_3$ or Np- Fe_3O_4 (F = 2.479 and p = 0.117/ F = 0.623 and p = 0.547, respectively), when compared to control group.

Micro-CT analysis

In order to construct grayscale graphics, we used the lower and upper threshold values by only selecting voxels within a histogram of all grayscale values of a given region of interest (ROI) that represented differences in the relationship from the control group, as represented in Figures 3a, 4a and 5a. After 24 and 96 h exposure, statistical differences were observed between the exposed groups and the control group, depending on the reading range observed in Figures 3a and 4a, respectively.

After 24 h of exposure to magnetite or maghemite, the ROI values in the 185 (F = 31.248; p < 0.001 and p < 0.01 for *post-hoc*, respectively) and the 200 (F = 8.169; p < 0.05 for *post-hoc*, to both NPs) ranges were statistically different compared to the control group.

Table 1 – Frequency of micronuclei and nuclear abnormalities in the peripheral blood erythrocytes of *Oriochromis niloticus* exposed to iron oxide nanoparticles.

Principal Group								
	Normal	Micronucleus	Bud	Binucleated	Blebbled	Lobed	Notched	Others
γ -Fe ₂ O ₃								
0 mg/L	94.7±3.4	0.0±0.0	0.1±0.1	0.0±0.0	2.1±1.7	0.5±0.4	2.5±1.7	0.1±0.1
25 mg/L	93.7±5.5	0.1±0.1	0.0±0.0	0.0±0.0	3.5±4.1	0.4±0.4	2.2±2.1	0.0±0.0
50 mg/L	98.1±0.8	0.0±0.0	0.0±0.0	0.0±0.0	1.4±0.8	0.2±0.2	0.4±0.4*	0.0±0.0
100 mg/L	98.2±0.7	0.0±0.0	0.0±0.0	0.0±0.1	1.1±0.5	0.2±0.1	0.4±0.2*	0.0±0.0
Fe ₃ O ₄								
0 mg/L	96.9±1.4	0.0±0.0	0.0±0.0	0.0±0.0	2.9±1.3	0.0±0.0	0.2±0.2	0.0±0.0
25 mg/L	98.1±2.0	0.0±0.0	0.1±0.1	0.0±0.0	0.5±0.5	0.2±0.2	1.1±1.3	0.0±0.0
50 mg/L	89.9±9.3	0.0±0.0	0.5±0.7*	0.0±0.0	6.4±6.7	1.1±1.1*	2.1±1.8	0.0±0.0
100 mg/L	97.5±0.8	0.0±0.0	0.0±0.0	0.0±0.0	1.2±0.7	0.8±0.3*	0.5±0.2	0.0±0.0
Satellite Group								
	Normal	Micronucleus	Bud	Binucleated	Blebbled	Lobed	Notched	Others
192 hours								
0 mg/L	97.2±1.5	0.0±0.1	0.0±0.0	0.0±0.0	0.7±0.4	0.8±0.6	1.2±0.7	0.0±0.0
100 mg/L (γ -Fe ₂ O ₃)	97.9±1.5	0.0±0.0	0.0±0.0	0.0±0.0	0.9±0.5	0.5±0.5	0.7±0.8	0.0±0.0
100 mg/L (Fe ₃ O ₄)	96.8±4.6	0.0±0.0	0.0±0.0	0.0±0.0	2.5±4.8	0.3±0.2	0.3±0.2*	0.0±0.1
288 hours								
0 mg/L	93.9±7.5	0.0±0.0	0.0±0.0	0.0±0.0	5.7±7.4	0.2±0.1	0.2±0.3	0.0±0.0
100 mg/L (γ -Fe ₂ O ₃)	98.7±0.6	0.0±0.0	0.0±0.0	0.0±0.0	0.6±0.4	0.3±0.2	0.4±0.3	0.0±0.0
100 mg/L (Fe ₃ O ₄)	97.7±0.6	0.1±0.1*	0.0±0.0	0.0±0.0	0.5±0.4	0.9±0.4*	0.8±0.5	0.0±0.0

Two thousand erythrocytes were read per fish (n=6/ subgroup) for analyze of the occurrence of micronuclei or nuclear abnormalities in these cells. The exposed groups (γ -Fe₂O₃ or Fe₃O₄) were evaluated in relation to the control group of each subgroup; whose statistical differences are represented by an asterisk (*), p<0.05. Data are represented by mean ± standard deviation (%). Principal Group – 96 hours post exposure of the test item; Satellite Group – 96 hours post exposure of the test item plus 96 or 192 hours of the additional recovery period (Total - 192 or 288 hours, respectively).

After 96 h of exposure to magnetite the ROI values in the 155 (F = 7.238; p < 0.05 for *post-hoc*), 170 (F = 15.508; p < 0.01 for *post-hoc*), 185 (F = 40.797; p < 0.001 for *post-hoc*), and 200 (F = 19.825; p < 0.05 for *post-hoc*) ranges also were statistically different to control group; whilst exposure to maghemite for the same time in the 170 (F = 15.508; p < 0.01 for *post-hoc*), 185 (F = 40.797; p < 0.001 for *post-hoc*), 200 (F = 19.825; p < 0.001 for *post-hoc*), 215 (F = 7.019; p < 0.05 for *post-hoc*), 230 (F = 7.125; p < 0.05 for *post-hoc*) and 245 (F = 7.781; p < 0.05 for *post-hoc*) ranges were statistically different compared to the control group.

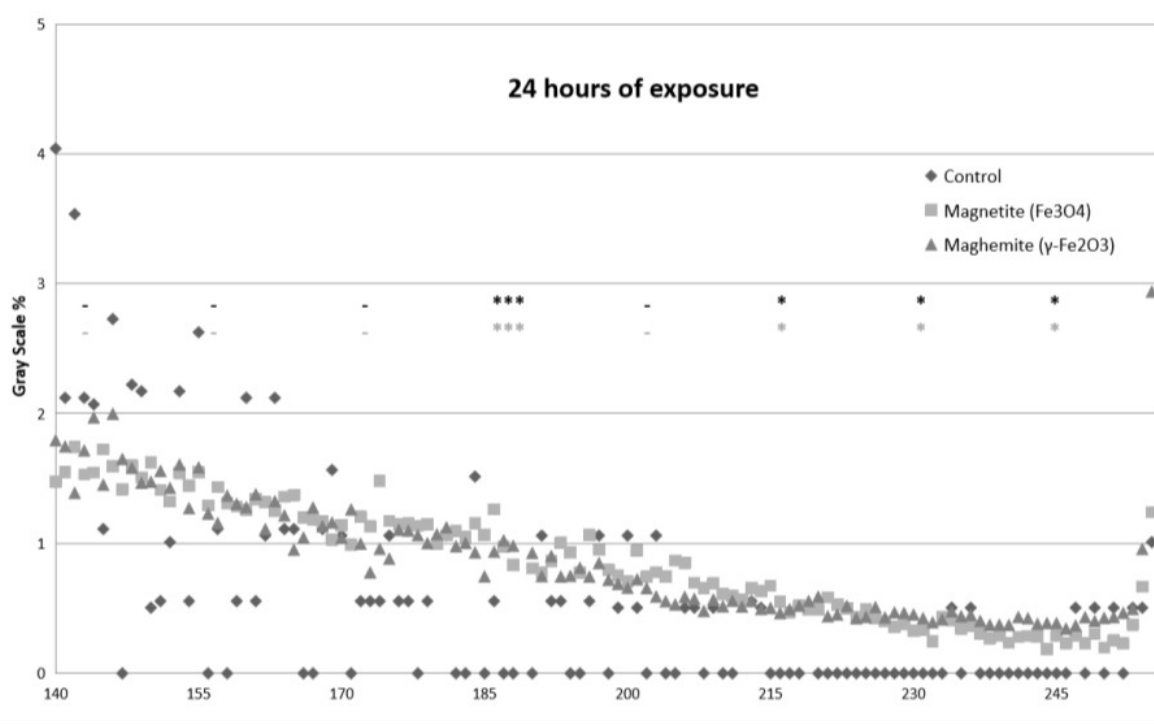
However, no significant differences were observed during recovery time (192 h) when exposure groups to magnetite or maghemite were both compared to control group, as depicted in Figure 6a (ROI-140: F = 0.743; ROI-155: H = 3.377; ROI-170: F = 1.142; ROI-185: F = 0.812; ROI-200: H = 3.396; ROI-215: H = 3.810; ROI-230: H = 1.667; ROI-245: H = 1.774; p > 0.05 for each F or H value).

Figures 3b and 4b present X-ray reconstructed images, showing FeO-NPs accumulation within the fish digestive system after exposure times of 24h (Figures 3b2 and 3b3) and 96h (Figures 4b2 and 4b3). We did not observe test-item accumulation after 192 h as supported in Figure 5b (b1, b2 and b3) or in the control group (Figures 3b1 and 4b1).

ICP-OES analysis

The total Fe content was measured by ICP-OES and expressed in mg Fe/kg of gill, hepatopancreas, kidney, muscle, and blood. As observed in Figure 6, fish exposed to maghemite showed an increase in Fe content at 96 h in the blood (6a), gill (6b), hepatopancreas (6c), and muscle (6e) in comparison to the control group (F = 7.691, H = 10.894, H = 9.877, H = 15.234, respectively; p < 0.05 for *post-hoc*, to all tissues) but not for fish exposed to magnetite (H = 6.887, H = 1.627, H = 2.000, H = 6.714, respectively; p > 0.05 for each H value); whilst statistical differences in iron concentration in the kidney (6d) were not observed in relation to the control group for both maghemite (F = 1.435 and p > 0.05) and magnetite (F = 2.011 and p > 0.05). On the other hand, we observed a statistically significant increased iron concentration in the blood (p < 0.01), gills (p < 0.05), hepatopancreas (p < 0.001), and muscle (p < 0.05) in the maghemite group compared to the magnetite group after 96 h; even though these values were not statistically different after 192 or 288 h (p > 0.05).

These results indicate tissue clearance after the 192 and 288 h recovery times, showing a similar Fe-content for all experimental groups (Figure 6). Regarding iron concentration in the gills, a comparison between groups exposed to NPs



a



Figure 3 – Grayscale graphic of X-ray microtomograph (a) and reconstructed images of tilapia-fishes (b1-3) exposure to $\gamma\text{-Fe}_2\text{O}_3$ or Fe_3O_4 for 24 h. b1: reconstructed images of control fish in 24 h exposure phase/b2: reconstructed images of fish exposed to $\gamma\text{-Fe}_2\text{O}_3$ / b3: reconstructed images of fish exposed to Fe_3O_4 . The data are represented by the mean of the grayscale values of a given region of interest (ROI), $n=3$ (per subgroup). Statistical differences are represented with asterisks (* $p<0.05$; *** $p<0.01$), in relation to the control group. The absence of significant difference is represented by a dash (- $p>0.05$). Top row (black) – Fe_3O_4 and bottom line (light gray) – $\gamma\text{-Fe}_2\text{O}_3$.

(6b) at 192 h showed statistical significance ($p < 0.01$) for the maghemite group, whose tissue clearance was observed after 288 h ($p > 0.05$).

Perl's Prussian Blue staining

The histological sections in Figure 7 show intestine (7a-f), hepatopancreas (7a, g-i) and gills (7 j-o) stained with Perl's Prussian Blue. Positive reactions to Perl's stain (blue) were observed: in the intestinal after 96 h exposure (7b, e $\gamma\text{-Fe}_2\text{O}_3$ or Fe_3O_4); and in the red cells and lamellae cells of the gills after 96 h exposure (7k, l $\gamma\text{-Fe}_2\text{O}_3$); in goblet cells, principally after 288 h recovery (7c, f $\gamma\text{-Fe}_2\text{O}_3$); Formalin-heme pigment were observed in hepatopancreas (7h-i) and between lamellae (7m) or gill arch (7n, o), mainly after exposure to $\gamma\text{-Fe}_2\text{O}_3$.

A positive reaction to Perl's stain in gills and hepatopancreas was observed in some animals exposed to

FeO-NPs; however statistically significant differences were observed in the maghemite group ($p < 0.001$); this positive and significant reaction was observed in the gills during all experimental period (Control = 6.25%; 96h = 83.3%; 192h = 85.7%; 288h = 57.143%), and, in the hepatopancreas, it was observed only at 96 h (Control = 4.8%; 96 h = 75.0%; 192 h = 0%; 288 h = 0%).

Besides, a positive reaction to Perl's stain in the lumen of the intestinal tract of animals exposed to maghemite ($p < 0.001$) was observed after the 96 h and 192 h exposures (Control = 0%; 96h = 83.3%; 192h = 50%; 288h = 0%); however, the exposure to magnetite caused an increase of the positive reaction ($p < 0.001$) only after the 96 h exposure (Control = 0%; 96h = 42.9%; 192h = 0%; 288h = 0%).

Moreover, a statistically significant increase in the positive reaction to Perl's Stain was observed in the intestinal

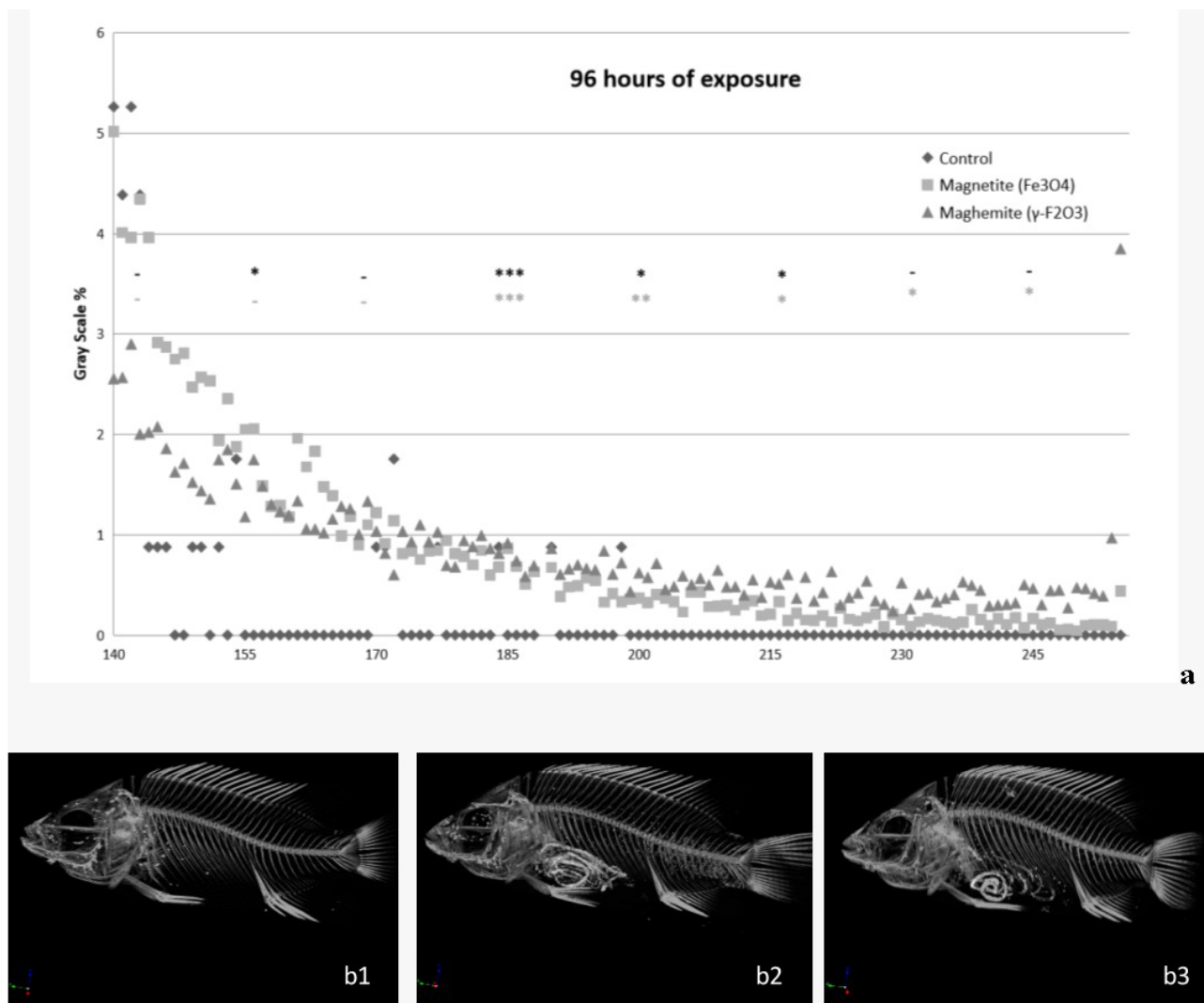


Figure 4 – Grayscale graphic of X-ray microtomograph (a) and reconstructed images of tilapia-fish (b1-3) exposed to $\gamma\text{-Fe}_2\text{O}_3$ or Fe_3O_4 for 96 h. b1:reconstructed images of control fish after 96 h of exposure phase/ b2: reconstructed images of fish exposed to $\gamma\text{-Fe}_2\text{O}_3$ / b3: reconstructed images of fish exposed to Fe_3O_4 . The data are represented by the mean of the grayscale values of a given region of interest (ROI), n=3 (per subgroup). Statistical differences are represented with asterisks (* p <0.05; ** p <0.01; *** p <0.01), in relation to the control group. Absence of significant difference is represented by a dash (- p >0.05). Top row (black) – Fe_3O_4 and bottom line (light gray) – $\gamma\text{-Fe}_2\text{O}_3$.

goblet cells ($p < 0.001$) of the group exposed to maghemite after 288 h (Control = 9.5%; 96h = 0%; 192h = 0%; 288h = 83.3%), despite the fact it was not statistically different after exposure to magnetite at all of the exposure times ($p > 0.05$).

Discussion

Fish are good indicators of metallic contamination in aquatic systems (Andreji *et al.*, 2005; Authman *et al.*, 2015). They are widely used as bio-indicators of metal pollution (Kumar *et al.*, 2011), and could therefore constitute a good metallic NP exposure indicator. Some materials could be accumulating in tissue and pose a health risk to those who frequently consume fish (Andreji *et al.*, 2005). In addition, this bioaccumulation could have adverse effects on the exposed organism, e.g. influence homeostasis and reproduction in fish; weaken the immune system and/or induce pathological changes (Authman *et al.*, 2015). Among this animal class, *Oreochromis* ssp (Tilapia) is an exotic fish species widely

cultivated in different countries for human consumption. These fish are able to accumulate certain environmental substances in their tissues, which could be correlated with human health risks (Jha, 2004; Bawuro *et al.*, 2018). On the other hand, there are few studies in the scientific literature using this species as a model to investigate the consequences of exposure to metallic-based NPs, including metal oxides, or other NMs.

Eighty articles papers were found in scientific databases (e.g. Science direct or PubMed) under ‘Tilapia’ or ‘*Oreochromis*’ and (‘nanomaterials’ or ‘nanoparticles’), as observed recently (December 2020). These studies report the adverse effects and/or accumulation of NMs in the fish species *Oreochromis niloticus* or *Oreochromis mossambicus* following chronic or acute exposure. Most of these studies analyzed inorganic NP exposure; e.g.: zinc oxide or metallic zinc NPs (Abdel-Khalek *et al.*, 2015; Alkaladi *et al.*, 2015; 2020; Kaya *et al.*, 2015; 2016; Farsani *et al.*, 2017; Abdelazim *et al.*, 2018; Anjugam *et al.*, 2018; Campos *et al.*, 2019;

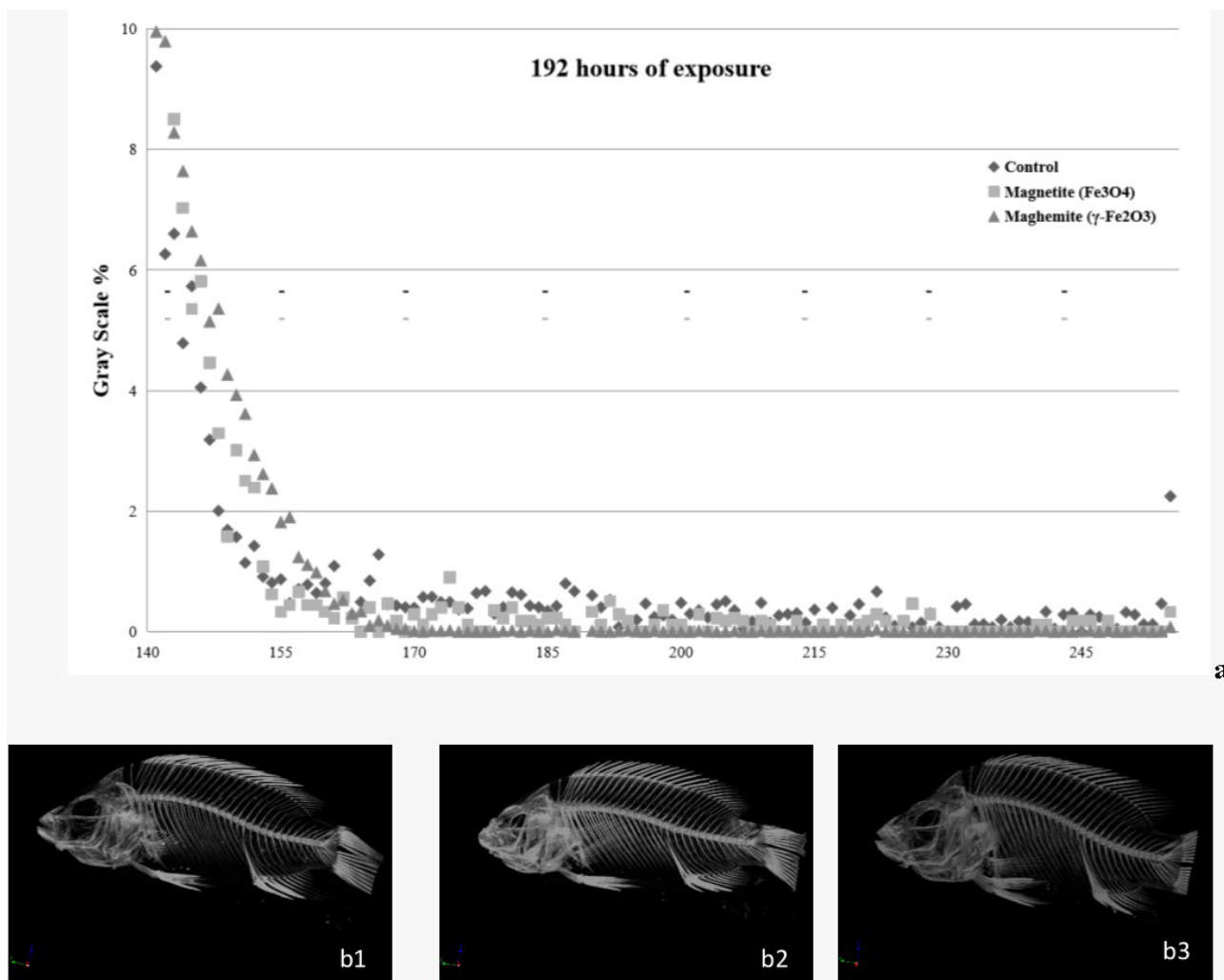


Figure 5 – Grayscale graphic of X-ray microtomograph (a) and reconstructed images of tilapia-fish (b1-3) at post-exposure phase (192 h after exposure to $\gamma\text{-Fe}_2\text{O}_3$ or Fe_3O_4 for 96 h). b1: reconstructed image of control fish in post-exposure phase/ b2: reconstructed image of fish exposed to $\gamma\text{-Fe}_2\text{O}_3$ in post-exposure phase/ b3: reconstructed images of fish exposed to Fe_3O_4 in post-exposure phase. The data are represented by the mean of the grayscale values of a given region of interest (ROI), $n=3$ (per subgroup). No statistical difference was observed ($p>0.05$). Top row (black) – Fe_3O_4 and bottom line (light gray) – $\gamma\text{-Fe}_2\text{O}_3$.

Suganthi *et al.*, 2019; Mohamed *et al.*, 2020) titanium oxide nanoparticles (Canli *et al.*, 2018; Suganthi *et al.*, 2019); silver nanoparticles (Govindasamy and Rahuman, 2012; Abu-Elala *et al.*, 2018; Ibrahim, 2020); aluminium oxide nanoparticles (Murali *et al.*, 2017; 2018; Abdel-Khalek *et al.*, 2020); gold nanoparticles (Vijayakumar *et al.*, 2017); cadmium nanoparticles or cadmium dioxide nanoparticles (Al-Abdan *et al.*, 2020; Ibrahim *et al.*, 2021); copper oxide nanoparticles (Abdel-Khalek *et al.*, 2015; Abu-Elala *et al.*, 2018; Shahzad *et al.*, 2018); nickel nanoparticles (Jayaseelan *et al.*, 2014), and iron oxide nanoparticles (Ates *et al.*, 2016; Abdel-Khalek *et al.*, 2020). At the same time, these species are widely used in aquaculture as a human source of protein there are few studies using tilapias as test-organism experimentally. So, tilapia-fish could be more explored in terms of their toxicological aspects or a potential source of NMs accumulated after environmental exposure.

In the present study, an increase in iron accumulation in the gastrointestinal tract of tilapia-fish after acute exposure (96 h) to the main forms of FeO-NPs - magnetite (Fe_3O_4) and its

oxidized form maghemite ($\gamma\text{-Fe}_2\text{O}_3$) – was observed, together with a subsequent decrease in iron content and recovery time. Hu *et al.* (2012) observed maghemite NP accumulation in the gut of *Ceriodaphnia dubia* after exposure to 5, 25 or 50 mg/L of nano- Fe_2O_3 , utilizing an optical microscope. In our study, Fe accumulation in the lumen of the digestive tract was detected utilizing X-ray computed microtomography after 24 h and 96 h, and by optical microscopy, when the contents in the lumen of the digestive tract reacted positively to Perl's reagent after 96 h exposure to FeO-NPs. Additionally, the presence of food in the digestive tract after 24 h exposure did not hinder observation of test-material accumulation in the organism, as observed in the grayscale graphic (Figure 3a) and the reconstructed images (Figures 3b2 and 3b3).

A similar study reported iron accumulation in the gastrointestinal tract of the Medaka larvae fish after exposure to 25–75 nm-sized magnetite NPs, with blue precipitation observed after Perl's reagent (Chen *et al.*, 2012). In the tilapia fish, accumulation in the lumen of the gastrointestinal tract was observed after 24 and 96 h (Figures 3, 4, 7b and 7e)

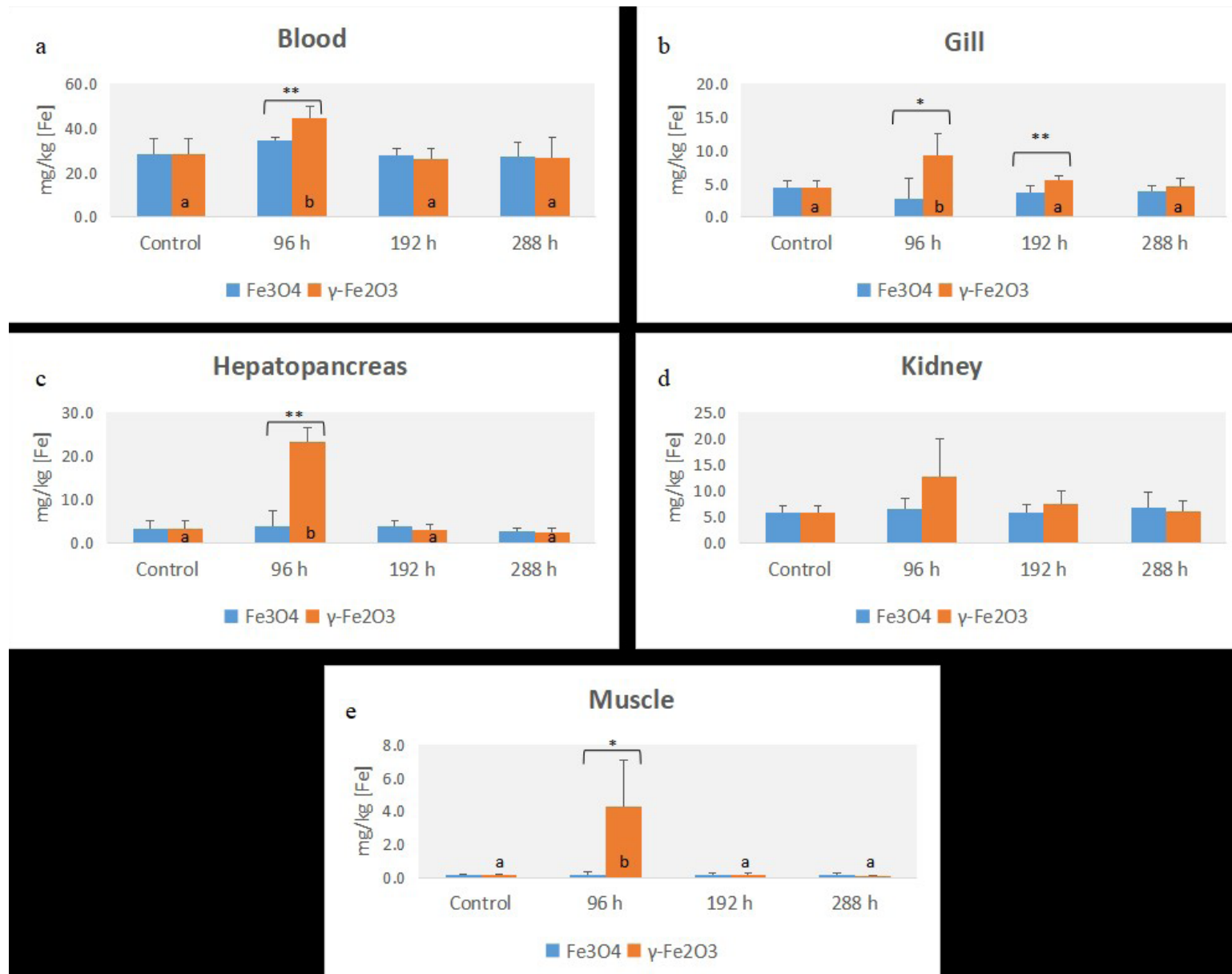


Figure 6 – Concentrations of iron content in blood, gill, hepatopancreas, kidney, and muscle (mg/Kg) after 96 h exposure to 0 or 100 mg/L iron oxide nanoparticles (γ -Fe₂O₃ or Fe₃O₄), at the end of exposure (96 h) or at the end of recovery time (192 h or 288 h). The data are represented by the mean \pm standard deviation, n=5 (per subgroup). Different letters (p<0.05) or asterisks (*p<0.05; **p<0.01) show statistical differences to the same nanoparticles at different times compared to the control or between different nanoparticles at the same time, respectively.

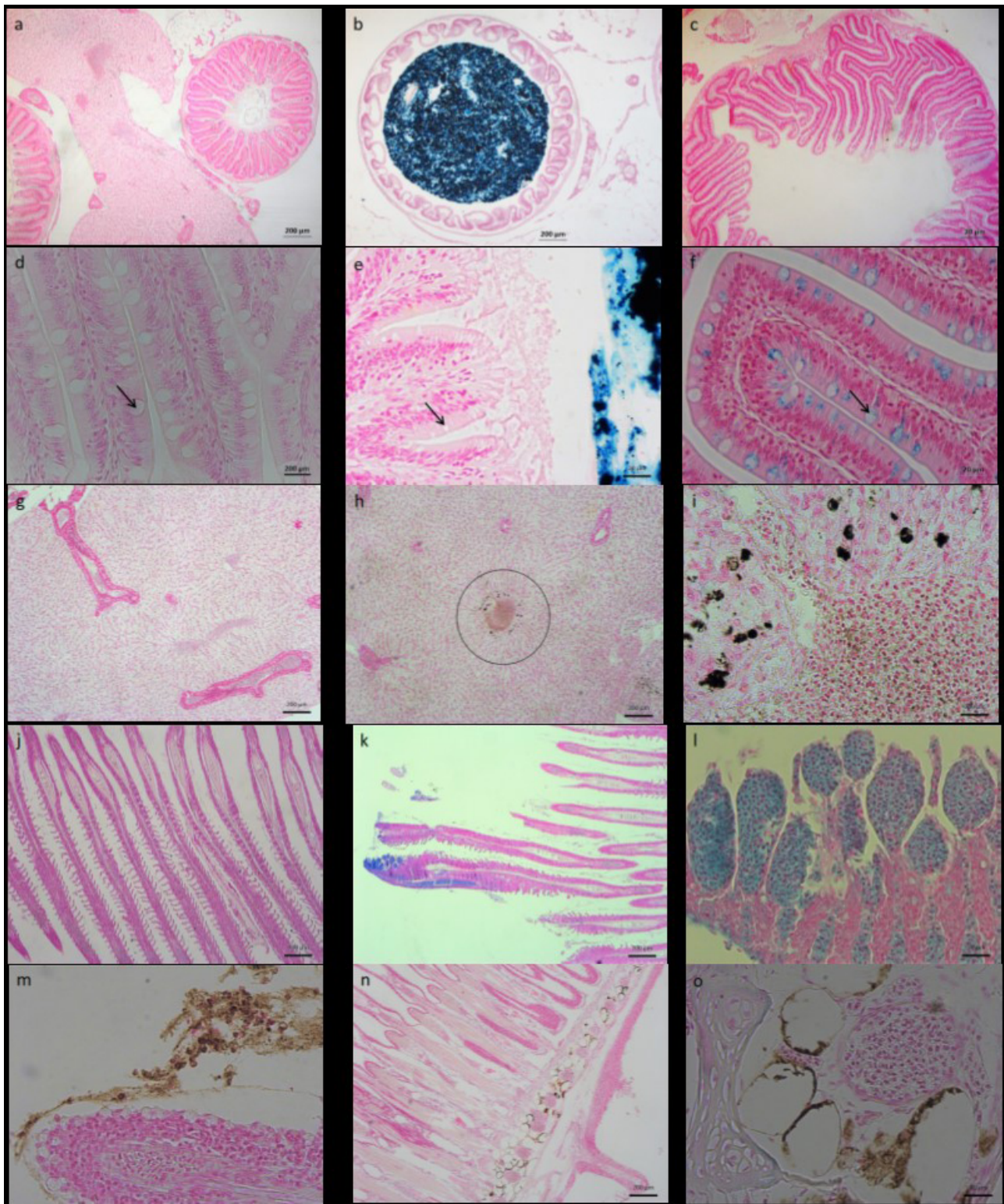


Figure 7 – Histological section showing gut and intestinal villi (a-f), hepatopancreas (a, g - i) and gills (j-o) after 96 h of exposure to 0 or 100 mg/L iron oxide nanoparticles ($\gamma\text{-Fe}_2\text{O}_3$ or Fe_3O_4), at the end of exposure (96 h) or at the end of recovery time (192 h or 288 h), (Perl's Stain). Control groups are represented in: a, d, g and j. Positive reaction to Perl's Stain (blue) was possible to observe: in lumen of the intestine after 96 h exposure (b and e $\gamma\text{-Fe}_2\text{O}_3$ or Fe_3O_4); and in the red cells and lamellae cells of the gills after 96 h exposure (k and l $\gamma\text{-Fe}_2\text{O}_3$); in goblet cells (arrows), principally after 288 h of recovery time (c and f $\gamma\text{-Fe}_2\text{O}_3$); formalin-heme pigment was observed in hepatopancreas (h - circle; i - detail of h circle) and between lamellae (m) or gill arch (n and o), mainly after exposure to $\gamma\text{-Fe}_2\text{O}_3$. This is a representation of the main findings found; the study was performed with n=5 slides/ per tissue/ per fish.

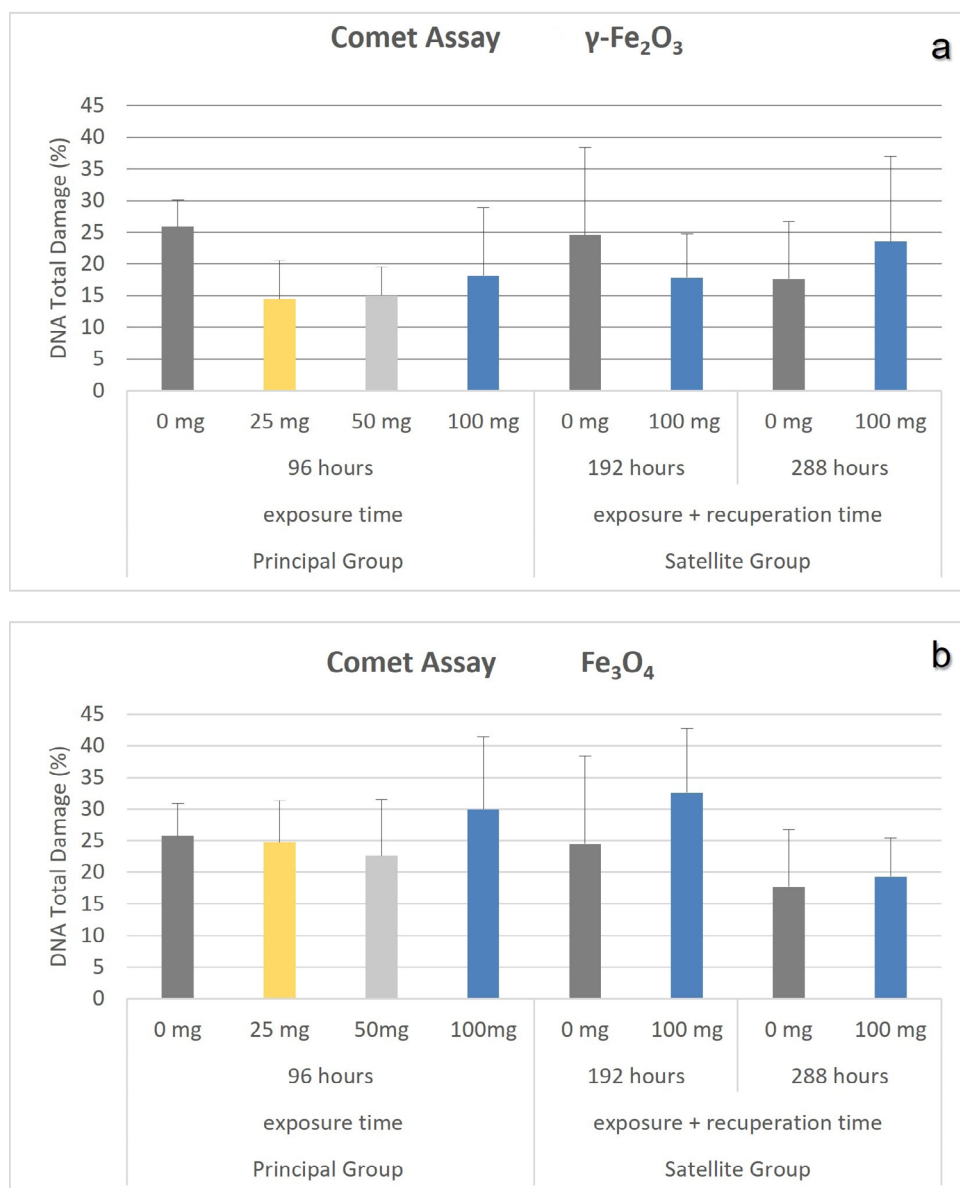


Figure 8 – DNA fragmentation (%) of the peripheral blood erythrocyte of *Oreochromis niloticus* exposed after 96 h exposure to iron oxide nanoparticles ($\gamma\text{-Fe}_2\text{O}_3$ or Fe_3O_4), at the end of exposure (96 h) or at the end of recovery time (192 h or 288 h). The data are represented by the mean \pm standard deviation, (n=6/subgroup). No statistical differences were observed after exposure or recovery time when compared to control, $p > 0.05$.

after exposure to $\gamma\text{-Fe}_2\text{O}_3$ or Fe_3O_4 NPs, but a reduced or absent accumulation was observed after the 192 h post-exposure phase, the period where fish were placed in clean water after exposure to NPs for 96 h (Figures 5 and 7). In this recovery time, the lumen of the digestive tract showed a reduced or absent reaction to Perl's and was negative in the micro-CT. A similar result was observed for *Ceriodaphnia dubia* (daphnia) following exposure to 20-40 nm Fe-NPs when this test organism was placed in a clean environment without NPs (Hu *et al.*, 2012).

Even in the absence of a positive Perl's reaction in the lumen of the digestive tract, a positive Perl's reaction was observed for goblet cells after the recovery period (Figures 7c and 7f), mainly in the time of 288 h for animals exposed to maghemite. Zhao *et al.* (2014) demonstrated that goblet cells are a natural pathway for NP excretion in zebrafish and

mice. Other authors also verified that metal NPs (*e.g.* silver nanoplates, magnetic Fe_3O_4 NPs, gold nanorods, and gold nanoclusters) injected via the tail were excreted into the gut lumen via the secretion of intestinal goblet cells (Liu *et al.*, 2019). From this perspective it was a similar observation to our study, an indication of depuration by goblet cells after oral exposure in a 192 or 288 h recovery time (Figures 7c and 7f).

As important as the excretion via is the route of exposure. There are 2 potential sites for metal uptake in fish, across the intestine (dietary borne) or branchial epithelium (water borne) (Bury and Grosell, 2003). Previously reported results, together with our data, show that the ingestion of FeO-NPs could be the main route of nanometal bioaccumulation in environmentally exposed organisms. We believe that exposure via the digestive tract was correlated with the increased iron concentration in the blood, hepatopancreas and muscle (Figures 6a, c, and e,

respectively). An interesting observation is that the increase in iron concentration was only present after 96 h of exposure to maghemite, and not for magnetite NP exposure. In the present study, γ -Fe₂O₃ was more readily taken up in acute exposure than Fe₃O₄ through the digestive tract and even by the respiratory tract epithelium. Moreover, this increased iron concentration returned to normal levels during the recovery time, similar to the control group, with the exception of the gills, whose clearance time was longer (Figure 6).

Some authors reported that FeO-NP uptake, distribution, clearance and toxicity depend on NP size and coating (Feng *et al.*, 2018). However, taking into account that the FeO-NPs utilized in this work are bare magnetite and maghemite NPs, similar in terms of size and morphology, our results indicate that the physicochemical characteristics of the NMs, such as composition, metal valence, surface and crystal properties can influence FeO-NP uptake by fish.

In fact, the structure of magnetite is that of an inverse spinel, with 32 O²⁻ ions regularly organized in a face-centered cubic unit cell with Fe³⁺ and Fe²⁺ ions distributed in octahedral and tetrahedral sites. The structure of maghemite is similar to that of magnetite, however, all or most Fe ions are in a trivalent state. To compensate the oxidation of Fe²⁺, the charge balance is achieved by cation vacancies in the structure (Peternele *et al.*, 2014). Thus, as expected, the XRD data of our samples confirm preservation of the spinel structure during the oxidation process (Figure 1). However, the easy oxidation of divalent iron ions in tetrahedral sites on the Fe₃O₄ surface (from the surface to the core) can change the properties of FeO-NPs, such as their surface reactivity (Schwaminger, *et al.*, 2017). Furthermore, Fe²⁺ ions occurring in magnetite are known to have an impact on the interaction of FeO-NPs with biological materials. For instance, maghemite commonly exhibits lower toxic effects than magnetite towards biological organisms (Auffan *et al.*, 2008; Auffan *et al.*, 2009).

Chen *et al.* (2012) related that exposure to zerovalent iron NPs resulted in gill iron deposition associated with mortality in medaka fish. In our study, a significant increase in iron content was observed in branchiate tissue after exposure to maghemite in comparison with the control (96 h) or with the magnetite group (96 h and 192 h). Some animals presented a positive reaction to Perl's stain, with altered staining of the erythrocyte cytoplasm or secondary lamellae cells (Figures 7k and l); other fish presented a formalin-heme pigment deposit between lamellae or the gill arch (Figure 7 m-o), without any significant statistical differences or mortality occurrence.

Iron is a vital micronutrient for teleost fish as it is an integral component of proteins involved in cellular respiration and oxygen transfer (Bury and Grosell, 2003; Andreji *et al.*, 2005). However, iron is toxic in excess, so fish need to balance uptake to prevent deficiency/potential toxicity (Bury and Grosell, 2003). The toxicity of iron-based NPs is a function of their properties, tolerance of test organisms and environmental conditions (Lei *et al.*, 2018). In our study, no clinical or behavioral abnormalities were observed in either the principal group or satellite group during or post-exposure to the test item.

A limited concentration of FeO-NPs was utilized (100 mg/L), as proposed by the OECD guideline - 203 (2019).

However, this guideline is not specific to evaluate exposure to nanomaterials. No morbidity or mortality was observed in the experimental groups, and the lethal concentration (LC₅₀) was higher than the concentration proposed as a test limit for chemicals. These data indicate that FeO-NPs present low toxicity to fish.

Appropriate physical and chemical characterization of natural and manufactured NPs is fundamental in order to determine their intrinsic properties. Phase purity, particle and cluster size, surface chemistry, solubility, charge and crystallinity are essential to elucidate the homogeneity, stability, reactivity, biodurability and potential application of NPs in different media (Peralta-Videa *et al.*, 2011). The solubility of FeO-NPs in water is extremely low (Brunner *et al.*, 2006). In our study, the γ -Fe₂O₃ or Fe₃O₄ NPs were insoluble and did not alter the physicochemical parameters of the water. Maghemite is more oxidized, and in a more stable iron oxide phase, than magnetite which could influence toxicity (Singh *et al.*, 2010). In the present study, differences in the oxidation grade of the NPs are not correlated with the occurrence of toxicity, but could be associated with differences in uptake after acute exposure. Metal bioconcentration and bioaccumulation processes depend on: the fish species and their trophic level, sampling location, type of food, type of absorption carried out by the organism, particle size, metal phase (dissolved or particulate) (Voigt *et al.*, 2015), and exposure time.

Zhang *et al.* (2015) and Ates *et al.* (2016) observed the accumulation and distribution of Fe or FeO-NPs in zebrafish (*D. rerio*) and tilapia-fish (*O. niloticus*), after chronic aqueous exposure to nano-Fe₂O₃, nano-Fe₃O₄, and α -Fe₂O₃ and γ -Fe₂O₃ NPs, respectively, using ICP-MS. After chronic exposure (60 days), tilapias were transferred to NP-free freshwater resulting in the elimination of ingested NPs within 30 days, except in the hepatopancreas and spleen (Ates *et al.*, 2016). After chronic waterborne exposure (52 days), the accumulated NPs were eliminated efficiently when fish were moved to NP-free water for 24 days post-exposure. According to Fe content analysis of fish excrement during the elimination phase, iron oxide NMs may be adsorbed via the gastrointestinal tract, and stored for more than 12 days (Zhang *et al.*, 2015).

The genotoxicity of iron-based NPs *in vivo* and *in vitro* from cellular level up to the whole organism are related to ROS-induced oxidative stress, which is the most accepted toxic mechanism (Lei *et al.*, 2018). The comet assay has been successfully used for detection of damages caused by oxidized DNA bases in fish exposed to environmental contaminants. The alkaline version offers increased sensitivity to agents that cause DNA oxidative lesions (Jha, 2008). In this study, comet assay correlates with micronucleus test and nuclear abnormalities, evidencing neither genotoxicity nor cytotoxicity. In conclusion, these results demonstrate that acute exposures to FeO-NPs promotes an increased iron-content in the fish's body during exposures, which rapidly returns to normal indices throughout the recovery period, with no apparent toxicity. On the other hand, *O. niloticus* can be tolerant to sublethal toxicity of FeO-NPs, developing increased activities of antioxidants enzymes, which were not quantified in this study.

Acknowledgements

Brazilian Ministry of Education – CAPES, Brazilian National Council for Scientific and Technological Development – CNPq and Nanobiotechnology INCT.

Conflicts of Interest

Authors declare there is no conflict or competing interests.

Author Contributions

MLF, CKG and RBA designed the *in vivo* experiments and interpreted the biological results. MLF, WG and MCF performed *in vivo* experiments, and collected and processed the samples for this study. MLF and MCF analyzed genotoxicity tests. MLF and PRCV processed the samples and WOP, and MHS obtained results for ICP-OES. FHH, PRCV and MLF processed the samples for histology. MLF and SBC obtained the images in X-ray computed microtomography. WSP synthesized and characterized the nanoparticles. MLF performed the statistical analysis and wrote the manuscript. CKG, RBA and MHS refined the article text. All co-authors contributed by commenting and approved the final manuscript.

References

- Abdelazim AM, Saadeldin IM, Swelum AA, Afifi MM and Alkaladi A (2018) Oxidative stress in the muscles of the fish Nile tilapia caused by zinc oxide nanoparticles and its modulation by vitamins C and E. *Oxid Med Cell Longev* 2018:6926712.
- Abdel-Khalek A, Kadry M, Hamed A and Marie AA (2015) Ecotoxicological impacts of zinc metal in comparison to its nanoparticles in Nile tilapia *Oreochromis niloticus*. *J Basic Appl Zool* 72:113-125.
- Abdel-Khalek AA, Badran SR and Marie M-AS (2020) The effective adsorbent capacity of rice husk to iron and aluminum oxides nanoparticles using *Oreochromis niloticus* as a bioindicator: Biochemical and oxidative stress biomarkers. *Environ Sci Poll Res Int* 27:23159-23171.
- Abu-Elala NM, Abubkr HO, Khattab MS, Mohamed SH, El-hady M, Ghandour RA and Morsi RE (2018) Aquatic environmental risk assessment of chitosan/silver, copper and carbon nanotube nanocomposites as antimicrobial agents. *Int J Biol Macromol* 1:1105-1115.
- Al-Abdan MA, Bin-Jumah MN and Alarifi S (2020) Exploration of cadmium dioxide nanoparticles on bioaccumulation, oxidative stress, and carcinogenic potential in *Oreochromis mossambicus* L. *Oxid Med Cell Longev* 26:5407159.
- Ali A, Zafar H, Zia M, Haq IU, Phull AR, Ali JS and Hussain A (2016) Synthesis, characterization, applications, and challenges of iron oxide nanoparticles. *Nanotechnol Sci Appl* 9:49-67.
- Alkaladi A, El-Deen NAMN, Afifi M and Zinadah OAA (2015) Hematological and biochemical investigations on the effect of vitamin E and C on *Oreochromis niloticus* exposed to zinc oxide nanoparticles. *Saudi J Biol Sci* 22:556-563.
- Alkaladi A, Afifi M, Ali H and Saddick S (2020) Hormonal and molecular alterations induced by sub-lethal toxicity of zinc oxide nanoparticles on *Oreochromis niloticus*. *Saudi J Biol Sci* 5:1296-1301.
- Al-Sabti K and Metcalfe CD (1995) Fish micronuclei for assessing genotoxicity in water. *Mutat Res* 343:121-135.
- Andreji J, Stránai I, Massányi P and Valent M (2005) Concentration of selected metals in muscle of various fish species. *J Environ Sci Health A, Tox Hazard Subst Environ Eng* 40:899-912.
- Anjugam M, Vaseeharan B, Iswarya A, Gobi N, Divya M, Thangaraj MP and Elumalai P (2018) Effect of β -1,3 glucan binding protein based zinc oxide nanoparticles supplemented diet on immune response and disease resistance in *Oreochromis mossambicus* against *Aeromonas hydrophila*. *Fish Shellfish Immunol* 76:247-225.
- Ashoka S, Peake BM, Bremmer G, Hageman KJ and Reid MR (2009) Comparison of digestion methods for ICP-MS determination of trace elements in fish tissues. *Anal Chim Acta* 653:191-199.
- Ates M, Demir V, Arslan Z, Kaya H Yilmaz S and Camas M (2016) Chronic exposure of tilapia (*Oreochromis niloticus*) to iron oxide nanoparticles: Effects of particle morphology on accumulation, elimination, hematology and immune responses. *Aquat Toxicol* 177:22-32.
- Auffan M, Achouak W, Rose J, Roncato M, Chaneac C, Waite D, Woicik J, Wiesner M and Bottero J (2008) Relation between the redox state of iron-based nanoparticles and their cytotoxicity toward *Escherichia coli*. *Environ Sci Technol* 42:6730-6735.
- Auffan M, Rose J, Bottero J-Y, Lowry GV, Jlivet J-P and Wiesner MR (2009) Towards a definition of inorganic nanoparticles from an environmental, health and safety perspective. *Nat Nanotechnol* 4:634-641.
- Authman MMN, Zaki MS, Khallaf EA and Abbas H (2015) Use of fish as bio-indicator of the effects of heavy metals pollution. *J Aquat Res Develop* 6:328.
- Bawuro AA, Voegborlo RB and Adimado AA (2018) Bioaccumulation of heavy metals in some tissues of fish in Lake Geriyo, Adamawa State, Nigeria. *J Environ and Pub Health* 2018:1854892.
- Boxall AB, Tiede K and Chaudhry Q (2007) Engineered nanomaterials in soils and water: How do they behave and could they pose a risk to human health? *Nanomedicine* 2:919-927.
- Brink NW, Kokalj AJ, Silva PV, Lahive E, Norrfors K, Baccaro M, Khodaparast Z, Loureiro S, Drobne D, Cornelis G *et al.* (2019) Tools and rules for modelling uptake and bioaccumulation of nanomaterials in invertebrate organisms. *Environ Sci Nano* 6:1985-2001.
- Brunner TJ, Wick P, Manser P, Spohn P, Grass RN, Limbach LK, Bruinink A and Stark WJ (2006) In vitro cytotoxicity of oxide nanoparticles: Comparison to asbestos, silica, and the effect of particle solubility. *Environ Sci Technol* 40:4374-4381.
- Bury N and Grosell M (2003) Iron acquisition by teleost fish. *Comp Biochem Physiol C Toxicol Pharmacol* 135:97-105.
- Campos RP, Chagas TQ, Alvarez TGA, Mesak C, Vieira JEA, Paixão CFC, Rodrigues SL, Menezes IPP and Malafaia G (2019) Analysis of ZnO nanoparticle-induced changes in *Oreochromis niloticus* behavior as toxicity endpoint. *Sci Total Environ* 682:561-571.
- Canli EG, Dogan A and Canli M (2018) Serum biomarker levels alter following nanoparticle (Al_2O_3 , CuO, TiO_2) exposures in freshwater fish (*Oreochromis niloticus*). *Environ Toxicol Pharmacol* 62:181-187.
- Chen PJ, Tan S-W and Wu W-L (2012) Stabilization or oxidation of nanoscale zerovalent iron at environmentally relevant exposure changes bioavailability and toxicity in medaka fish. *Environ Sci Technol* 46:8431-8439.
- Elijah JP, Diamond SA, Kennedy J, Goss GG, Ho K, Lead J, Hanna SK, Hartmann NB, Hund-Rinke K, Mader B *et al.* (2015) Adapting OECD aquatic toxicity tests for use with manufactured nanomaterials: Key issues and consensus recommendations. *Environ Sci Technol* 49:9532-9547.

- Farré M, Gajda-Schratz K, Kantiani L and Barceló D (2009) Ecotoxicity and analysis of nanomaterials in the aquatic environment. *Anal Bioanal Chem* 393:81-95.
- Farsani HG, Doria HB, Jamali H, Hasanpour S, Mehdipour N and Rashidiyan G (2017) The protective role of vitamin E on *Oreochromis niloticus* exposed to ZnONP. *Ecotoxicol Environ Saf* 145:1-7.
- Feng Q, Liu Y, Huang J, Chen K, Huang J and Xiao K (2018) Uptake, distribution, clearance, and toxicity of iron oxide nanoparticles with different sizes and coatings. *Sci Rep* 8:2082.
- GHS (2019) Globally Harmonized System of Classification and Labelling of Chemicals. ST/SG/AC.10/30/Rev8, 570 p.
- Govindasamy R and Rahuman AA (2012) Histopathological studies and oxidative stress of synthesized silver nanoparticles in Mozambique tilapia (*Oreochromis mossambicus*). *J Environ Sci* 24:1091-1098.
- Hu J, Wang D, Wang J and Wang J (2012) Bioaccumulation of Fe₂O₃ (magnetic) nanoparticles in *Ceriodaphnia dubia*. *Environ Pol* 162:216-222.
- Ibrahim ATA (2020) Toxicological impact of green synthesized silver nanoparticles and protective role of different selenium type on *Oreochromis niloticus*: Hematological and biochemical response. *J Trace Elem Med Biol* 61:126507.
- Ibrahim ATA, Banae M and Sureda A (2021) Genotoxicity, oxidative stress, and biochemical biomarkers of exposure to green synthesized cadmium nanoparticles in *Oreochromis niloticus* (L.). *Comp Biochem Physiol C Toxicol Pharmacol* 242:108942.
- Jayaseelan C, Rahuman AA, Ramkumar R, Perumal P, Rajakumar G, Kirithi ASV, Santhoshkumar T and Marimuthu S (2014) Effect of sub-acute exposure to nickel nanoparticles on oxidative stress and histopathological changes in Mozambique tilapia, *Oreochromis mossambicus*. *Ecotoxicol Environ Saf* 107:220-228.
- Jha AN (2004) Genotoxicological studies in aquatic organisms: An overview. *Mutat Res* 552:1-17.
- Jha AN (2008) Ecotoxicological applications and significance of the comet assay. *Mutagenesis* 23:207-221.
- Kaya H, Aydin F, Gurkan M, Yilmaz S, Ates M, Demir V and Arsla Z (2015) Effects of zinc oxide nanoparticles on bioaccumulation and oxidative stress in different organs of tilapia (*Oreochromis niloticus*). *Environ Toxicol Pharmacol* 40:936-947.
- Kaya H, Aydin F, Gurkan M, Yilmaz S, Ates M, Demir V and Arsla Z (2016) A comparative toxicity study between small and large size zinc oxide nanoparticles in tilapia (*Oreochromis niloticus*): Organ pathologies, osmoregulatory responses and immunological parameters. *Chemosphere* 144:571-582.
- Kumar B, Mukherjee DP, Kumar S, Mishra M, Prakash D, Sing SK and Sharma S (2011) Bioaccumulation of heavy metals in muscle tissue of fishes from selected aquaculture ponds in east Kolkata wetlands. *Annals Biol Res* 2:125-134.
- Lei C, Sun Y, Tsang DCW and Lin D (2018) Environmental transformations and ecological effects of iron-based nanoparticles. *Environ Pol* 232:10-30.
- Liu Y, Liu K, Yang M, Han Y, Zang Q, Conde J, Yang Y, Alfranca G, Wang Y, Ma L *et al.* (2019) Gastric parietal cell and intestinal goblet cell secretion: A novel cell-mediated *in vivo* metal nanoparticle metabolic pathway enhanced with diarrhea via chinese herbs. *Nanoscale Res Lett* 14:79.
- Mohamed AS, Soliman HA and Ghannam HE (2020) Ameliorative effect of vitamins (E and C) on biochemical alterations induced by sublethal concentrations of zinc oxide bulk and nanoparticles in *Oreochromis niloticus*. *Comp Biochem Physiol C Toxicol Pharmacol* 242:108952.
- Morais PC, Garg VK, Oliveira AC, Silva LP, Azevedo RB, Silva AML and Lima ECD (2001) Synthesis and characterization of size-controlled cobalt-ferrite-based ionic ferrofluids. *J Magnetism Magnetic Mater* 225:37-40.
- Murali M, Suganthi P, Bukhari AS, Mohamed HES, Basu H and Singhal RK (2017) Histological alterations in the hepatic tissues of Al₂O₃ nanoparticles exposed freshwater fish *Oreochromis mossambicus*. *J Trace Elem Med Biol* 44:125-131.
- Murali M, Athif P, Suganthi P, Bukhari AS, Mohamed HES, Basu H and Singhal RK (2018) Toxicological effect of Al₂O₃ nanoparticles on histoarchitecture of the freshwater fish *Oreochromis mossambicus*. *Environ Toxicol Pharmacol* 59:74-81.
- Nowack B and Bucheli TD (2007) Occurrence, behavior and effects of nanoparticles in the environment. *Environ Pol* 150:5-22.
- Oberdörster G, Maynard A, Donaldson K, Castranova V, Fitzpatrick J, Ausman K, Karn B, Wolfgang K, Lai D, Olin S *et al.* (2005) Principles for characterizing the potential human health effects from exposure to nanomaterials: Elements of a screening strategy. *Part Fibre Toxicol* 2:8.
- OECD (2019) Test n. 203: Fish, acute toxicity test. Guidelines for the testing of chemicals, section 2. OECD Publishing, Paris.
- Ostiguy C, Roberge B, Ménard L and Endo CA (2009) A good practice guide for safe work with nanoparticles: The Quebec Approach. *J Phys Conf Ser* 151:012037.
- Patil US, Adireddy S, Jasiwal A, Mandava S, Lee BR and Chrisey DB (2015) *In vitro/in vivo* toxicity evaluation and quantification of iron oxide nanoparticles. *Int J Mol Sci* 16:24417-24450.
- Peralta-Videa JR, Zhao L, Lopez-Moreno M, La Rosa G, Hong J and Gardea-Torresdey JL (2011) Nanomaterials and the environment: A review for the biennium 2008–2010. *J Hazard Mater* 186:1-15.
- Peterlele WS, Fuentes VM, Fascineli ML, Silva JR, Silva RC, Lucci CM and Azevedo RB (2014) Experimental investigation of the coprecipitation method: An approach to obtain magnetite and maghemite nanoparticles with improved properties. *J Nanomater* 2014:682985.
- Pomeroy M, Brun NR, Peijnenburg WJGM and Vjver MG (2017) Exploring uptake and biodistribution of polystyrene (nano) particles in zebrafish embryos at different developmental stages. *Aquat Toxicol* 190:40-45.
- Schwaminger SP, Bauer D, Fraga-Garcia P, Wagner FE and Berensmeier (2017) Oxidation of magnetite nanoparticles: Impact on surface and crystal properties. *Cryst Eng Comm* 19:246-255.
- Shahzad K, Khan MN, Jabeen, F, Kosour N, Chaudhry AS and Sohail M (2018) Evaluating toxicity of copper(II) oxide nanoparticles (CuO-NPs) through waterborne exposure to tilapia (*Oreochromis mossambicus*) by tissue accumulation, oxidative stress, histopathology, and genotoxicity. *Environ Sci Pol Res Int* 25:15943-15953.
- Silva MP, Drummond AL, Aquino VRR, Silva LP, Azevedo RB, Sales MJA, Morais PC, Bakuzis AF and Sousa MH (2017) Facile green synthesis of nanomagnets for modulating magnetohyperthermia: Tailoring size, shape and phase. *RSC Adv* 7:47669-47680.
- Singh N, Jenkins GJS, Asadi R and Doak SH (2010) Potential toxicity of superparamagnetic iron oxide nanoparticles (SPION). *Nano Rev* 1:5358.
- Singh NP, McCoy MT, Tice RR and Schneider EL (1988) A simple technique for quantitation of low levels of DNA damage in individual cells. *Exp Cell Res* 175:184-191.

- Sousa MH, Silva GJ, Depeyrot J, Tourinho FA and Zara LF (2011) Chemical analysis of size-tailored magnetic colloids using slurry nebulization in ICP-OES. *Microchem J* 97:182-187.
- Suganthi P, Murali M, Athif P, Bukhari AS, Mohamed HES, Basu H and Singhal RK (2019) Haemato-immunological studies in ZnO and TiO₂ nanoparticles exposed euryhaline fish, *Oreochromis mossambicus*. *Environ Toxicol Pharmacol* 66:55-61.
- Teja AS and Koh PY (2009) Synthesis, properties, and applications of magnetic iron oxide nanoparticles. *Progress Crystal Growth Characteriz* 55:22-45.
- Valdiglesias V, Kiliç G, Costa C, Fernández-Bertólez, Pásaro E, Teixeira JP and Laffon B (2015) Effects of iron oxide nanoparticles: Cytotoxicity, genotoxicity, developmental toxicity, and neurotoxicity. *Environ Mol Mutagenesis* 56:125-148.
- Vijayakumar S, Baskaralingam V, Balasubramanian M, Gobi N, Ravichandran S, Karthi S, Ashokkumar B and Sivakumar N (2017) A novel antimicrobial therapy for the control of *Aeromonas hydrophila* infection in aquaculture using marine polysaccharide coated gold nanoparticle. *Microb Pathog* 110:140-151.
- Voigt CL, Silva CP, Doria HB, Randi MAF, Ribeiro CAO and Campos SX (2015) Bioconcentration and bioaccumulation of metal in freshwater neotropical fish *Geophagus brasiliensis*. *Environ Sci Pol Res* 22:8242-8252.
- Wang WX and Rainbow PS (2008) Comparative approaches to understand metal bioaccumulation in aquatic animals. *Comp Biochem Physiol C Toxicol Pharmacol* 148:315-23.
- Zhang Y, Zhu L, Zhou Y and Chen J (2015) Accumulation and elimination of iron oxide nanomaterials in zebrafish (*Danio rerio*) upon chronic aqueous exposure. *J Environ Sci* 30:223-230.
- Zhao B, Sun L, Zhang W, Wang Y, Zhu J, Zhu X, Yang L, Li C, Zhang Z and Zhang Y (2014) Secretion of intestinal goblet cells: A novel excretion pathway of nanoparticles. *Nanomedicine* 10:839-849.

Associate Editor: Carlos R. Machado

License information: This is an open-access article distributed under the terms of the Creative Commons Attribution License (type CC-BY), which permits unrestricted use, distribution and reproduction in any medium, provided the original article is properly cited.